

Experimental investigations of heat transfer and pressure drop during the condensation process within plate heat exchangers of the herringbone-type[☆]

Reinhard Würfel^{*}, Nikolai Ostrowski

Martin-Luther-Universität Halle-Wittenberg, Fachbereich Ingenieurwissenschaften, 06099 Halle, Germany

Received 2 September 2002; accepted 7 April 2003

Abstract

The application of compact heat exchangers to the realization of the processes with phase change gaseous-liquid is increasingly significant. However, the state of the knowledge is unsatisfactory for modelling the heat transfer and the pressure drop. Experimental investigations for condensation in channels of corrugated plates of a plate heat exchanger were carried out with the condensing vapours water and n-heptane. The loads of the vapour phase as well as the kind of the plate corrugation were used as experimental parameters. The results to the heat transfer coefficient and friction pressure drop refer to the condition of a complete condensation. An essential influence of the phase load as well as of the corrugation inclination angle is observed in the investigated range of the shear controlled two-phase flow. The intensity of heat transfer increases with a factor of approx. 3–4, compared to the calculation of the Nusselt theory of the laminar film. A discussion of the experimental data was realized on base of modelling of the turbulent two phase channel flow.

© 2003 Elsevier SAS. All rights reserved.

Zusammenfassung

Die Anwendung von kompakten Wärmeübertragern zur Realisierung von Prozessen mit Phasenänderung gasförmig-flüssig gewinnt zunehmend an Bedeutung. Allerdings ist der Wissensstand zur Modellierung der Wärmeübergangsintensität und des Druckverlustes unbefriedigend. Es wurden experimentelle Untersuchungen zur Kondensation in geprägten Kanälen eines Platten-Wärmeübertragers mit den kondensierenden Dämpfen Wasser und n-Heptan durchgeführt. Die Dampfbelastung sowie die Art der Plattenprägung wurden als experimentelle Parameter verwendet. Die erhaltenen Ergebnisse zum mittleren Wärmeübergangskoeffizient und Reibungsdruckverlust beziehen sich auf die Bedingung einer vollständigen Kondensation. Im untersuchten Bereich einer scherkraft-kontrollierten Zweiphasenströmung wird der wesentliche Einfluß der Phasenbelastung sowie des Plattenprägewinkels deutlich. Die Intensität des Wärmeüberganges erhöht sich auf das 3–4 fache im Vergleich zur Modellrechnung einer laminaren Filmtheorie nach Nusselt. Ein Modellvorschlag auf der Basis einer turbulenten Zweiphasenströmung wurde zur Korrelation der experimentellen Daten verwendet.

© 2003 Elsevier SAS. All rights reserved.

Keywords: Plate heat exchanger; Condensation; Heat transfer; Pressure drop; Experiment; Turbulent flow; Corrugation inclination angle

Schlüsselwörter: Plattenwärmeübertrager; Kondensation; Wärmeübergang; Druckverlust; Experiment; turbulente Strömung; Prägewinkel

1. Introduction

In the use of heat exchangers there is an increasing tendency to apply compact apparatuses with heat transfer characteristics, such as the realization of high heat transfer coef-

ficients and the countercurrent flow between the fluids. Further, large heat transfer surfaces can be placed in limited apparatus volumes. However, the necessarily raised consumption of energy for the compensation of the occurring friction pressure drop is often disadvantageous. The plate heat exchanger (PHE) meets the requirements of such a compact apparatus. It can be successfully applied in liquid phases in combination with a lot of technical heat transfer processes. In connection with the realization of many technical heat transfer processes a successful application of the PHE is pos-

[☆] On the basis of a presented paper by R. Würfel at the GVC-meeting to heat and mass transfer, March 2001 in Bamberg, Germany.

^{*} Corresponding author.

E-mail address: reinhard.wuerfel@iw.uni-halle.de (R. Würfel).

Nomenclature

b	width of the plate.....	m
d	diameter.....	m
F_A	enhancement factor of the area	
g	acceleration due to gravity.....	$\text{m}\cdot\text{s}^{-2}$
$\Delta^{LV}h$	specific latent heat of condensation....	$\text{J}\cdot\text{kg}^{-1}$
L	length of the plate.....	m
\bar{m}	mass flux.....	$\text{kg}\cdot\text{m}^{-2}\cdot\text{s}^{-1}$
Nu	Nusselt number, $= \frac{\alpha \cdot d_h}{\lambda}$	
Pr	Prandtl number	
Δp	pressure drop.....	Pa
Re_V	Reynolds number of the vapour, $= \frac{\bar{m}_V \cdot d_h}{\eta_V}$	
Re_L	Reynolds number of the condensate (or liquid), $= \frac{\bar{m}_L \cdot d_h}{\eta_L}$	
s	gap of the plate.....	m
T, t	temperature.....	K, °C
X_{LM}	Lockart–Martinelli-parameter	
x	vapour quality in Eqs. (8) and (13); length in mean stream direction.....	m

Greek symbols

α	heat transfer coefficient.....	$\text{W}\cdot\text{m}^{-2}\cdot\text{K}^{-1}$
α^*	normalized heat transfer coefficient, $= \alpha_L(\gamma)/\alpha_L(45^\circ)$	
δ	thickness.....	m
Φ	two phase flow multiplier	
γ	corrugation inclination angle.....	degree

η	dynamic viscosity.....	$\text{kg}\cdot\text{m}^{-1}\cdot\text{s}^{-1}$
λ	heat conductivity.....	$\text{W}\cdot\text{m}^{-1}\cdot\text{K}^{-1}$
ρ	density.....	$\text{kg}\cdot\text{m}^{-3}$
ξ	friction coefficient of single phase	

Indices

acc	acceleration
c	cooling water
cal	calculated
cr	critical
co	condensation
eq	equivalent
exp	experimental
F	friction
grav	gravitation
hp	<i>n</i> -heptan
h	hydraulic
in	input
L	liquid
m	average value
Nus	Nusselt film model
out	output
p	plate
t	total
V	vapour
W	wall
wa	water

sible in liquid phases. Compared to the heat transport intensity in smooth channels, a 3- to 4-fold heat transfer coefficient can be achieved, due to local changes of flow direction as well as of the flow velocity and consequently the renewal of the boundary layer in narrow channels with corrugated plates.

The utilization of PHE increasingly occurs in the field of transport processes during gas–liquid phase changes [1]. It is also used in condensation applications in process and refrigeration industries. The efficiency depends on applying the advantages of liquid systems to the conditions of the specific two-phase flow. In principle it is known how to intensify heat transfer—as for instance during the film condensation—by means of passive methods without supplying additional energy [2]. Accordingly, the following methods are known, for the conditions with essential transfer resistances in the condensate film.

- the increase of the interfacial shear stress,
- the roughness of the heat transfer area,
- ribbed or corrugated surfaces (Gregory-effect),
- inserts of static mixers in the flow channel.

These passive effects of the augmentation of the transfer intensity can occur, when the condensation process is realized in PHE with corrugated plates. Regardless of it, only some studies have been published on experimental data and on modelling heat transfer as well as the friction pressure drop in a condensation process in PHE. Table 1 shows a qualitative comparison of the contents of various previous publications. Most of the experimental studies are referred to the working systems water and refrigerants. The geometrical quantities of the used experimental channels are indicated only partially. However, they allow the assumption, that the investigated corrugated plates were employed with industrial dimensions. The kind of the chosen plates mostly corresponds to the herringbone-type with the measuring range of the corrugation inclination angle $\gamma = 30^\circ - 60^\circ$ and of the middle gap between the plates $s = 2.5 - 7.4$ mm. The authors mainly described experimental results of input–output-investigations. The chosen fluid loads were characterized by the Reynolds number of the liquid phase in the total range $80 < Re_L < 2000$. Obviously, the criterion for the transition of the laminar into the turbulent flow ($Re_{L,cr}$) depends on the chosen plate geometry [1]. Generally, the chosen modelling

correlations describing the heat transfer during the condensation in the vertical corrugated plate channel correspond to the model propositions as applied in vertical smooth tubes or channels. In dependence on the mass flux of the phases two characteristic flow fields can be defined.

- The gravity controlled flow regime is characterized by a small influence of the vapour phase on the hydrodynamics of the liquid flow at low mass fluxes. The liquid flow is separated from the vapour flow [1]. The Nusselt laminar film theory is the basis for the calculation of heat transfer in the condensate.
- In contrast, there are significant interactions between gaseous and liquid phases in case of the shear controlled flow regime at high mass fluxes. Often the modelling of heat transfer is realized by characteristic parameters of the two-phase flow in the channel.

The experimental results from various works (see Table 1) were correlated mainly with these modelling proposals. A further article [16] presents a study on heat transfer in condensation of pure and mixtures of hydrocarbons in a compact welded PHE. For low Reynolds numbers ($Re_L < 100$), the condensation occurs almost filmwise and for

higher values of Re_L the modeling of a two-phase channel flow is used. The transition between the two regimes is between $Re_L = 100$ and 1000 and depends on the operating conditions. The modelling of the condensation of multi-component mixtures in PHE is also described by [17] with the help of semi-empirical equations.

Fig. 1 shows a comparison of the calculations by different authors about the mean heat transfer characteristic for the condensation of organic vapours. Hereby, considerable deviations are evident. Obviously the validity of these correlations is limited to the test conditions. Therefore own experimental investigations were carried out in the field of heat transfer and pressure drop of the condensation process in a vertical corrugated plate channel, both for aqueous and organic working systems.

2. Experimental apparatus and operating conditions

The aim of these works was to discuss the influence of different physical properties, of fluid loads and of the corrugation inclination angle of the plates on the intensity of heat transport and pressure changes. Fig. 2 shows a simplified scheme of the experimental plant used. The condensing medium flows in the closed circuit and in the range of the

Table 1
Experimental investigations of condensation processes in plate channels by various authors

Author	Working system	Heat transfer area of the plate [m ²]	Corrugation inclination angle γ [grad]	Flow characteristic	Channel gap s [mm]	Kinds of modelling
Kumar [3]	NH ₃ R22		brazed plates			flow of condensate film
Wang [4]	H ₂ O	0.045	type BR-05; herringbone pattern of 45°	$Re_{L,cr} \approx 200$	≈ 2.5	flow of condensate film
Panchal [5]	NH ₃	1.8×0.82	30°; 60°	gravity-controlled	≈ 4	flow of condensate film
Nakaoka [6]	R22	2.15×0.24	$\approx 30^\circ$	flooding of condensate film	≈ 5	channel flow with influence of free convection
Di-an [7]	H ₂ O	0.27×0.08	0°; 45°	$Re_{L,cr} = 350$	5	flow of condensate film
Müller Steinhagen [8,9]	air -H ₂ O	0.32×0.1	alfa-laval (P01; P20) 60°; 90°		2.4	two-phase-channel flow
Yan [10]	R 134a	0.45×0.12	60°	$Re_L = 500-1000$	3.3	two-phase-channel flow
Tovazhnyanski [11]	H ₂ O	1.1×0.3	30°; 60°	$Re_L > 300$	5	two-phase-channel flow
Chopard [12]	R 22	1.28×0.15	smooth or corrugated and studded plates	Forced convection	$\approx 3.8-4.5$	two-phase-channel flow
Wang, Sunden [13]	H ₂ O	0.75×0.25	30°	$Re_L = 800-1800$	≈ 5	two-phase-channel flow
Wang, Christensen [14]	H ₂ O	0.032–0.5	30°; 45°; 60°	$Re_L = 300-2000$	4.8–7.4	modified Boyko/Kruzhilin-equation
Cheng [15]	H ₂ O	1×0.8	type BRS08; (made in P.R. China)	$Re_L = 80-180$	5.8	flow of condensate film

normal pressure. The experimental plant was heated by superheated steam. Both evaporator (1) and condensation testing unit (2) were carried out as a plate apparatus of industrial construction and dimension. The control of the mass flow rate for the heating steam allowed to adjust the inlet state of the condensable vapour into unit (2) as a small superheated steam. The experimental plant was sufficiently heat-insulated and the circulation of the condensing medium was realized by a proportioning piston pump (5). The condensing testing unit was built as a 3-channel system with two cooling channels. In this way, the real conditions of heat transport in the plate package of an industrial PHE were realized approximately. Coolant (water) and condensing vapour existed in the countercurrent flow. The input- and output-data of pressure, temperature and the mass flow rate

of the plate channels were measured during the complete investigations. Thus an integral evaluation became possible. Due to the choice of a 3-channel system, the recording of the local measuring information is complicated. However, the heat-insulated testing unit allowed information regarding the local temperatures of the coolant by measuring the corresponding wall temperatures T_W of the external channel plates. Dimensions of the employed corrugated plates and the 15 measuring points for determining T_W are represented in Fig. 3. The heat transfer area is given by the dimension of the base plate $L \times b = 0.56 \text{ m} \times 0.19 \text{ m}$.

The chosen type of the corrugated plate corresponds to the herringbone corrugation pattern. The definition of the inclination angle γ (see Fig. 3) related to the axis of the main direction of flow. Within the plate package,

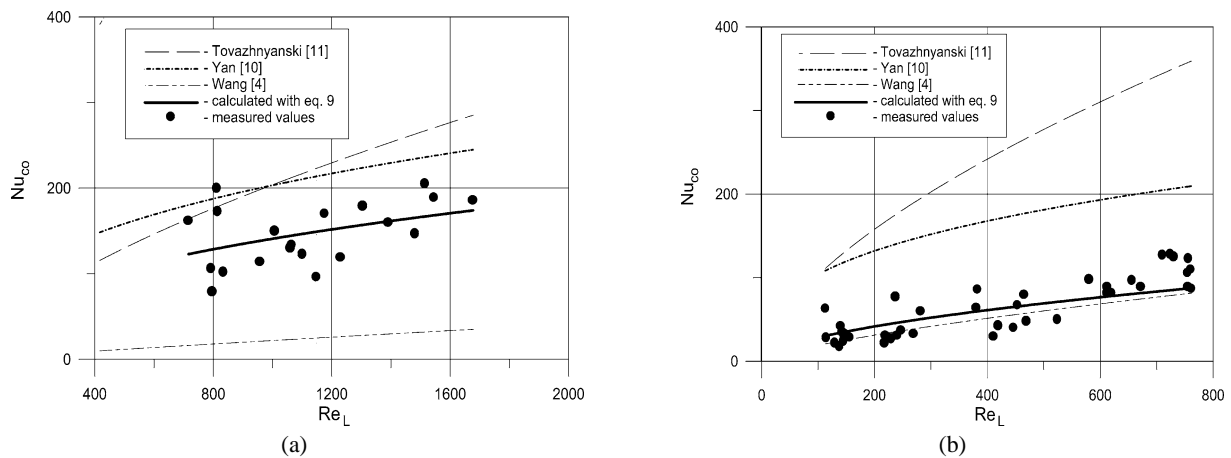


Fig. 1. Comparison of own experimental and—according to various correlations—calculated average dimensionless heat transfer coefficients of the condensation, Nu_{CO} dependent on Re_L in PHE, (a) *n*-heptane; plate combination h/h; (b) water; plate combination l/l.

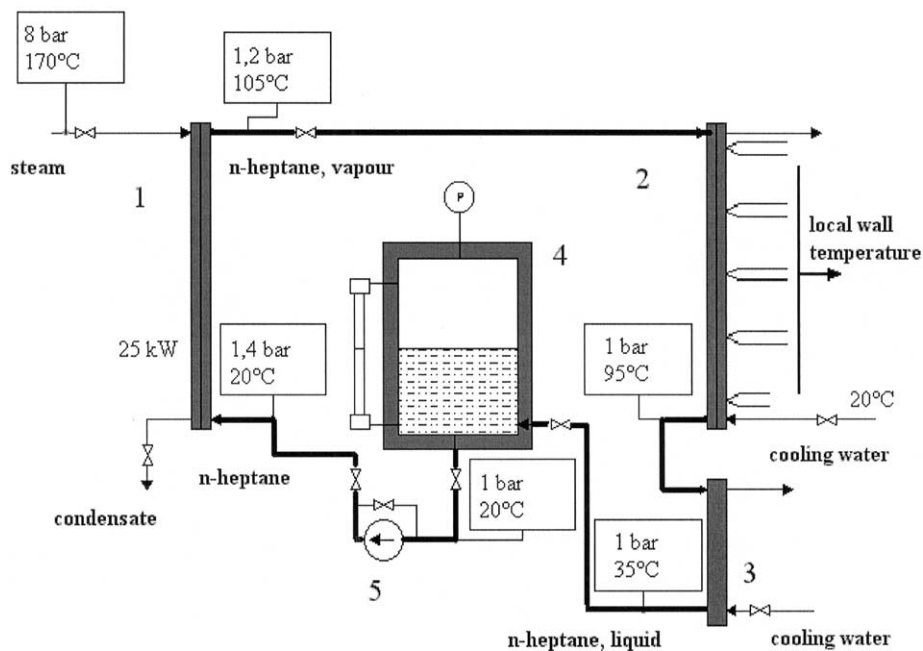


Fig. 2. Simplified scheme of the experimental plant; 1—evaporator (PHE); 2—condensation testing unit (PHE); 3—cooler (Shell and tube heat exchanger); 4—storage tank; 5—proportioning pump.

the neighboring plates were turned by 180°. Thereby the plates were in contact with themselves in the area of the wave crest. The complete experimental investigations of the condensation process were carried out in a plate channel under the following operating conditions (see Table 2).

The following geometrical parameters (see Table 3) correspond to the different corrugated plates.

It is to be expected that an increase in the inclination angle γ in the corrugated plate channel effects an enlargement of the drag. Therefore in accordance the definitions by other authors the plates with $\gamma = 30^\circ$ are denoted as “low (l)” and the plates with $\gamma = 60^\circ$ as “high” (h). The knowledge of the heat flow distribution along the main direction of flow x is a precondition to determine the experimental heat transfer coefficients which represent the zone of the condensation process. For example, Fig. 4 shows the behaviour of local cooling water temperatures T_C at the measuring points in accordance with Fig. 3. Depending on the location of the thermocouple along the plate width b , a non-negligible de-

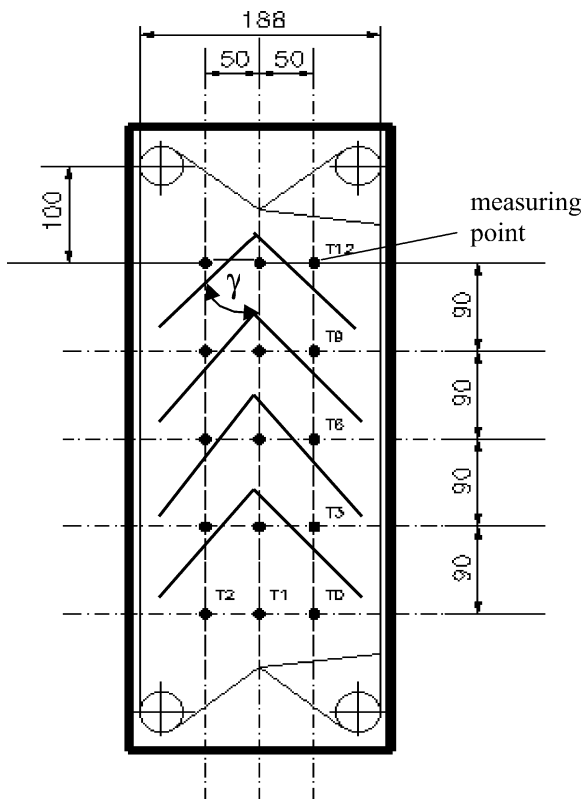


Fig. 3. Simplified pattern of the experimental corrugated plate and measuring points of wall temperatures; γ = corrugation inclination angle.

viation becomes visible. These local differences can be connected with the hydrodynamically different conditions (for example, the phase distribution) normal to the main direction of flow. A further evaluation is not possible, because additional local measuring information is not available. Therefore, an axially local average temperature $T_{C,x}$ was determined. Knowing the complete integral measuring data of the condensing medium as well as its saturated temperature T^{LV} , a comparison of the heat balances succeeds at a maximum error of approx. $\pm 3\%$. Thus the necessary area for transferring the heat of condensation and superheating can be determined for all test conditions. Fig. 4 shows an example of the qualitative temperature characteristic of the condensing medium as well as of the cooling water to the complete phase change. Generally, the conditions of a complete condensation was realized during all the experiments.

The information about the temperature characteristic of the streaming phases and of the heat flow along the length of the plate channel allows the determination of the experimental overall heat transfer coefficients k_{CO} . In general, difficulties exist to measure the wall temperature T_W in the compact channel system. Therefore, information on the heat transfer coefficient of the condensing phase becomes possible provided that the transport behaviour in the coolant is known.

For this reason, the heat transfer behaviour between two liquid fluids without condensation was examined with the available measuring unit and analogous geometrical conditions of the plates. The fluids *n*-heptane and water were

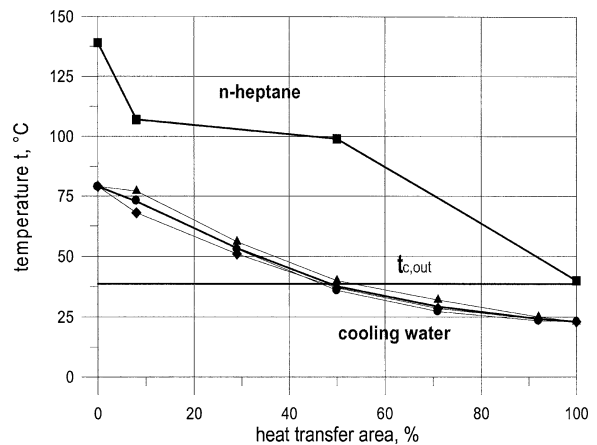


Fig. 4. The experimental temperature characteristics of the cooling water (various measuring points across the width of the plate, see Fig. 2) and condensing *n*-heptane depending on the channel length; $t_{c,out}$ = temperature of the cooling water at the end of the condensation.

Table 2
Experimental parameter range of condensation in the 3-channel plate system

Condensing medium	Water			<i>n</i> -heptane		
$Re_{L,out}$	110–900			350–1650		
$Re_{V,in}$	2500–19000			9500–4500		
γ of the neighbouring plates	30°/30°	30°/60°	60°/60°	30°/30°	30°/60°	60°/60°
kind of plate installation	l/l	l/h	h/h	l/l	l/h	h/h

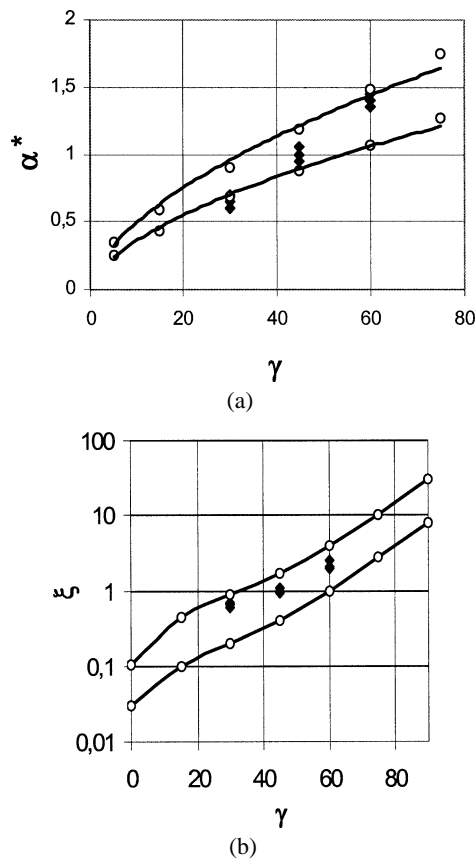


Fig. 5. The normalized heat transfer coefficient α^* (a) and the friction coefficient ξ (b) for a liquid flow in PHE versus γ according to a diagram by [18]; ($Re_L \approx 2000$) • our own measured data; —○—○— range of experimental data in [18].

Table 3
Geometrical parameters of the used corrugated plates

Inclination angle γ	30°/(l)	60°/(h)
d_h in mm	6.3	3.4
with plate installation	(l/l)	(h/h)
Enhancement factor of the heat transfer area F_A	$\sim 1,141$	$\sim 1,093$

also used as working systems. It can be assumed, that the same model correlation is valid for both fluids to describe the mean convective heat transfer in the liquid phase. Therewith a modelling is possible on the basis of integral measuring information (see Eqs. (1)–(3)).

$$\frac{1}{k_L} = \frac{1}{\alpha_{L,wa}} + \frac{\delta_p}{\lambda_p} + \frac{1}{\alpha_{L,hp}} \quad (1)$$

$$\alpha_{L,wa} = \frac{Nu_{L,wa} \cdot \lambda_{L,wa}}{d_h}; \quad \alpha_{L,hp} = \frac{Nu_{L,hp} \cdot \lambda_{L,hp}}{d_h} \quad (2)$$

$$Nu_L = C_1 \cdot Re_L^{C_2} \cdot Pr_L^{0.33} \quad (3)$$

with $C_1, C_2 = f$ (geometry of the plates).

The experimental investigations to single-phase heat transfer and pressure drop were carried out in the field of turbulent flow ($\approx Re_L > 350$ in PHE). A comparison of our own measuring data of α_L and the friction pressure drop $\Delta p_{F,L}$

with a modelling proposal after [18] was made by the help of dimensionless quantities α^* and ξ . The normalized heat transfer coefficient α^* and the friction factor ξ (see also Eq. (10)) are shown in dependence on the inclination angle. (See Fig. 5.) The boundary lines mark the field of various experimental results of other authors for different liquids [18]. The investigated experimental data can be classified in this field. Therefore the description of the heat transfer coefficient in coolant was performed on the basis of Eqs. (1)–(3), connected with the evaluation of all experiments for heat transfer in condensation.

3. Experimental results

Consequently the determination of the mean heat transfer coefficients α_{co} for the field of a total condensation follows with Eq. (4)

$$\frac{1}{\alpha_{co}} = \frac{1}{k_{co}} - \frac{1}{\alpha_c} - \frac{\delta_p}{\lambda_p} \quad (4)$$

Generally the experimental condition $(T_{V,in} - T^{LV}) < 30$ K was valid, and therefore the assumption can be taken, that the beginning of the condensation process is at the entry of the plate channel. Consequently, the values of k_{co} include additionally the sensible heat flow for superheated vapour. The accuracy of α_{co} is influenced by the quality of the experimental k_{co} and α_c .

It is known, the choice of the experimental channel system connects with its realization and the expenditure of systematical experimental investigations. Further, a transmissibility of experimental results to the conditions of the industrial PHE should be possible with sufficient accuracy. The advantage of a two-channel-system consists in a better realization of the local measuring informations. However, an essential disadvantage is that there occur heat-engineering and therefore hydrodynamic deviations from the real system because of the “one-direction”-heat transfer of the condensation channel. Fig. 6 shows values measuring of the heat transfer behaviour in the condensing phase, comparably for the conditions of the “one- and two-direction” heat transfer. The description of the dimensionless heat transfer coefficient Nu_{co} explains deviations depending on the fluid load (Re_L). In the field of the turbulent flow ($Re_L \geq 300$) differences are rather smaller than in the laminar flow. Obviously, the effect of the formed condensate films superposes itself also in the field of laminary flow, for the present condition of very narrow plate channels and the “two-direction”-heat transfer.

All subsequently discussed experimental results refer exclusively to a measuring unit with a “two-direction”-heat transfer. This arrangement corresponds more directly to the heat transfer conditions of the technical PHE. Figs. 7(a), (b) show the mean heat transfer coefficients α_{co} depending on the Reynolds-number of the condensate Re_L for different geometries and combinations of the plates. An important uniform influence of the Re_L can be seen in the whole range

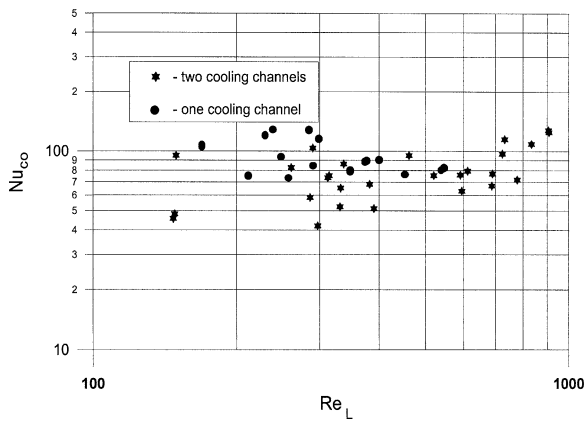


Fig. 6. Experimental Nu_{co} versus Re_L under different heat transfer conditions; condensing fluid: water; plate combination: h/h.

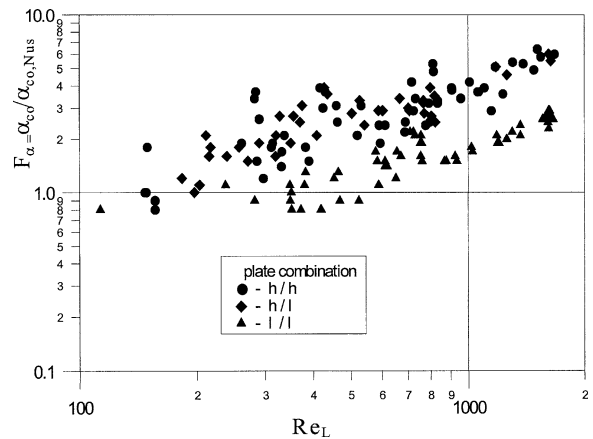
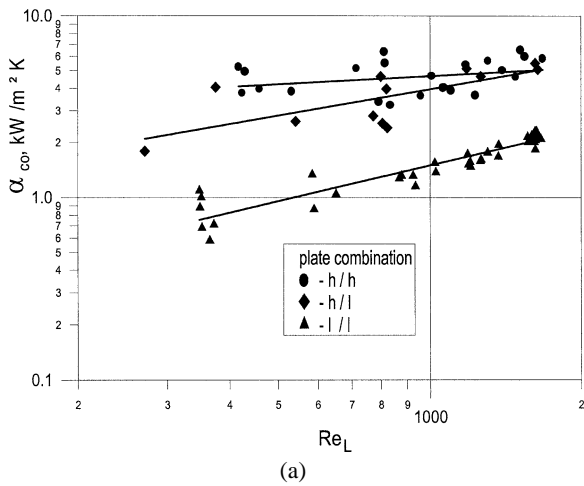
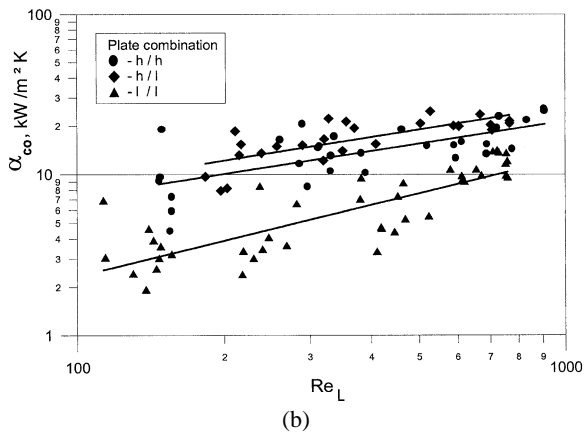


Fig. 8. Reduced experimental heat transfer coefficient $F_\alpha = \alpha_{co}/\alpha_{co,Nus}$ in various plate combinations dependent on Re_L ; condensing fluids: *n*-heptane, water.



(a)



(b)

Fig. 7. Experimental average heat transfer coefficients α_{co} in various plate combinations dependent on Re_L ; (a) *n*-heptane; (b) water.

of the phase loadings, both for the organic system *n*-heptane and for water. The characteristic of the graph is typical of the situation of a channel flow in the case of the forced convection and corresponds especially to the field of the turbulent film flow. The influence of the corrugation inclination angle γ is also significant. Accordingly a considerably higher heat transfer intensity can be achieved with the plate combina-

tion h/h than with the plate combination l/l. The increase of the transfer coefficients with a factor of approx. 3–4 for both investigated fluid systems corresponds to an effect which is also known for the heat transfer of the liquid phase flow in PHE. Consequently it can be assumed that the heat transfer behaviour during the condensation of pure media in the channel of corrugated plates is determined particularly by the characteristic liquid flow. The specific transfer behaviour of the plate combination h/l is remarkable. Figs. 7(a), (b) show an approximation of the corresponding α_{co} -values to the level of the channel geometry h/h. A further discussion of the experimental data of heat transfer allows the comparison in Fig. 8. The relation $F_\alpha = \alpha_{co}/\alpha_{co,Nus}$ characterizes the deviation of the real heat transport behaviour in the plate channel from a model calculation of the Nusselt film theory for condensation at vertical smooth walls (Eq. (5)).

$$\alpha_{co,Nus} = 0.943 \left(\frac{\rho_L \cdot (\rho_L - \rho_V) \cdot g \cdot \Delta^{LV} h \cdot \lambda_L^3}{\eta_L \cdot (T^{LV} - T_W) \cdot L} \right)^{0.25} \quad (5)$$

The significant influence of Re_L as well as the chosen plate combination can be seen analogously to Fig. 7. The range of value of the relation F_α results in $1 \leq F_\alpha \leq 7$ for the complete parameter range, with a maximum relative error of the experimental data of approx. $\pm 8\%$. Accordingly the intensity of the heat transfer increases significantly in the corrugated plate channel, compared with the modelling assumption of a laminar film condensation. Consequently, the experimental condition $F_\alpha \rightarrow 1$ results from the limiting value $Re_{L,out} \rightarrow 0$. Therewith, qualitative indications for the modelling strategy can be derived out of Fig. 8. Obviously, the heat transfer may be described by a film model of condensate in the field of smaller mass flux of the condensing medium ($Re_L < 250$). Higher liquid loadings in the two-phase flow of the narrow plate channel require another modelling strategy.

In the case of a high pressure drop, the industrial use of the PHE as a compact condenser with intensive heat transfer behaviour is not advisable. For the described experimental

conditions, the total pressure change Δp_t was measured along the channel length. The friction pressure drop Δp_F can be determined according to Eq. (6).

$$\Delta p_t = \Delta p_{\text{grav}} + \Delta p_{\text{acc}} + \Delta p_F \quad (6)$$

Here the hydrostatic pressure drop Δp_{grav} and acceleration pressure drop Δp_{acc} were calculated approximatively under mean condensation conditions considering of the supercooling zone (see Fig. 4). Due to the realization of a complete condensation, information about the behaviour of the local vapour void fraction ε_V are not necessary. The condition $(|\Delta p_{\text{grav}}| + |\Delta p_{\text{acc}}|)/|\Delta p_t| \leq 0.15$ could be maintained in the total experimental range. The friction pressure drop $|\Delta p_{\text{CO},F}|$ of the condensation is shown in Figs. 9(a), (b), dependent on Re_L and the geometry of the plate channel. In this case, $|\Delta p_{\text{CO},F}|$ contains the total pressure change of the vapour in the entry zone of the plate channel. The investigations for both fluid systems show analogous tendencies. Qualitatively, an interrelation between heat transport and the behaviour of the friction pressure drop can be seen. The significant influence of the fluid loading (Re_L) is visible as well as that of the corrugation angle γ . The arrangement of the $|\Delta p_{\text{CO},F}|$ -curve of the plate combination h/l is noteworthy again. In contrast to the behaviour of the heat transfer (see

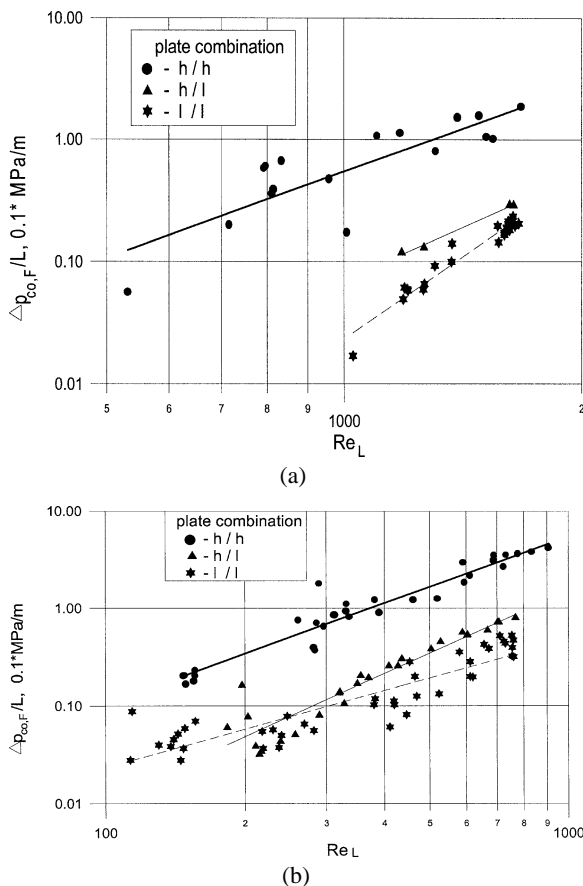


Fig. 9. Experimental friction pressure drop of the condensing field $\Delta p_{\text{CO},F}/L$ in various plate combinations dependent on Re_L (a) *n*-heptane, (b) water.

Fig. 7) the pressure drop approaches to the level of the plate combination l/l.

Generally, important higher friction pressure drops are found in the plate combination h/h. An application of this kind of the plate corrugation of the condensation processes appears problematic in the field of normal pressure and vacuum, independent of the intensive heat transfer. In contrast, the channel geometry h/l proves to be an optimal variant of the thermal and hydrodynamic point of view. In principle, the pressure range, determining for the experimental Δp_t was defined by measuring points of the inlet- and outlet-pipes near the plate channel. Thus, an important part of the pressure drop results in the section of the entry vapour flow, which is characterized by an essential change of the channel cross-section area. It is useful to compare our own experimental results with published models of other authors. However, the correlations of the two-phase flow in PHE, represented in some actual studies, refer to specific fluid systems and plate geometries (see Table 1). Furthermore, the geometric data of the plate channels and fields of the phase loadings are specified only partially or incompletely. With that, the determination of ranges of validity is problematic.

Fig. 1 shows a comparison of some model equations which calculate the mean heat transfer during the condensation. Generally, considerable deviations between experimental data and model calculations are to be found. However, a satisfactory agreement can be achieved with the correlation after Wang and Zhao [4] for the system water (see Fig. 1(b)) Hereby our own experimental conditions correspond to those of the model description. For condensation of *n*-heptane, the deviations are considerably higher, referring to a correlation after Yan and Lio [10], which was determined for the refrigerant R 134a (see Fig. 1(a)).

A comparison to the friction pressure drop $\Delta p_{\text{CO},F}$, specified in Fig. 10, also shows great deviations between model calculations and own experimental data. The differently defined pressure range of Δp_t can be an essential reason. This

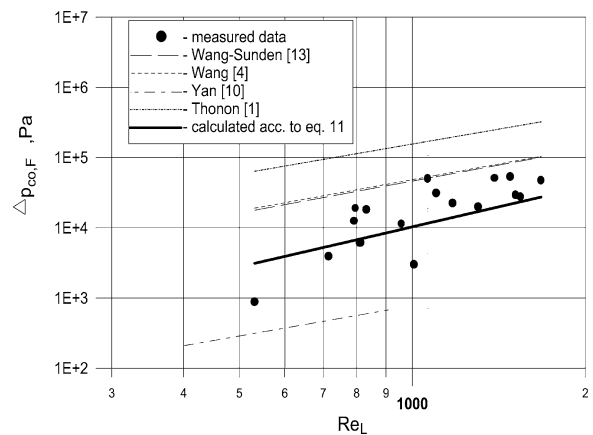


Fig. 10. Comparison of experimental and—according to various correlations—calculated friction pressure drop $\Delta p_{\text{CO},F}$ of the condensation in PHE; condensing fluid: *n*-heptane; plate combination: h/h.

becomes particularly problematic in the processes with non-adiabatic two-phase flow, as in the present case.

4. Model description

Due to the restricted usefulness of modelling in actual literature, our own correlations how to describe the experimental data about heat transfer and friction pressure drop, will be discussed. The investigated range of phase loadings (see Table 2) allows the assumption that a turbulent flow of the gas–liquid-system exists in the profiled plate channel. A shear-controlled regime is decisive for the momentum and heat transport processes [1]. Obviously, the turbulent flow in the narrow rectangular channel is not characterized by a separation from liquid and vaporous phase (non separated two-phase flow). The hydraulic Reynolds number Re_h , which is proposed by other authors [4,10], is used for characterizing of the special two-phase system (Eq. (7)).

$$Re_h = \frac{G_{eq} \cdot d_h}{\eta_L} \quad (7)$$

G_{eq} , as modified equivalent mass flux, is defined in accordance with Eq. (8).

$$G_{eq} = \bar{m} \left[(1-x) + x \left(\frac{\rho_L}{\rho_V} \right)^k \right] \quad (8)$$

Therefore the description of the average dimensionless heat transfer coefficients of condensation can be proposed by Eq. (9).

$$Nu_{co} = C \cdot Re_h^m \cdot Pr_L^{0.33} = \frac{\alpha_{co} \cdot d_h}{\lambda_L}, \quad \text{where } x = x_m = 0.5 \quad (9)$$

Consequently, the significant influence of the convective heat transport in the liquid flow is explained. The constants C , m and k depend on the geometry of the corrugated plates. They were determined on the basis of the correlation with the inclusion of all measuring data for the systems waters and *n*-heptane (see Table 4).

Figs. 1 and 11 show the comparison of the measured and according to Eq. (9) calculated data of Nu_{co} . A model description with a maximum relative error of 30% is achieved for approx. 90% of all experimental data.

A simple correlation on the basis of the modelling type by Lockart–Martinelli (LM) was chosen for the description of our own experimental data about the friction pressure drop of condensation $\Delta p_{K0,F}$. The application of this modelling was often used to estimate the friction pressure drop of various adiabatic two phase flow gas–liquid in channels [4,9,13,19].

In principle, the calculation was realized on the basis of a single-phase flow. For instance, the liquid phase friction pressure drop of the single plate channel can be calculated as follows (see Eq. (10)).

$$\Delta p_{L,F} = \left(\bar{m}_L^2 \cdot L \cdot \xi / (2 \cdot \rho_L \cdot d_h) \right) \quad (10)$$

Information according to Fig. 5(b) can be included into a discussion of ξ , because the modelling equation after [18] is useful for the experimental channel geometries in sufficient accuracy. The connection between local $\Delta p_{CO,F}$ and $\Delta p_{L,F}$ is defined corresponding to Lockart–Martinelli by a two-phase multiplier Φ (see Eq. (11)).

$$\Delta p_{CO,F} = \Phi^2 \cdot \Delta p_{L,F} \quad (11)$$

Φ is formulated as a function of the LM-parameter X_{LM} .

$$\Phi^2 = F \cdot X_{LM}^{-2} \quad (12)$$

The single phase—friction coefficient ξ can be calculated according to the Blasius approach for turbulent flow conditions of both phases. Also, Eq. (13) is valid for turbulent—turbulent flow.

$$X_{LM} = \left(\frac{1-x}{x} \right)^{0.9} \cdot \left(\frac{\rho_V}{\rho_L} \right)^{0.5} \cdot \left(\frac{\eta_L}{\eta_V} \right)^{0.1} \quad (13)$$

The correlation of all experimental data on the integral friction pressure drop during the total condensation ($x = x_m = 0.5$) produced a necessary dependence of the constant factor F on the plate geometry (see Table 5).

Fig. 12 shows a comparison of measured and according to Eq. (11) calculated $\Delta p_{CO,F}$ of the investigated working systems. A model description is achieved with a maximum relative error of 30% for approx. 85% of the experimental data.

Table 4
Constants according to Eq. (9), depending on the plate combination

Combination of the plates	C	m	k
h/h	3.77	0.43	0.14
h/1	3.2	0.46	0.3
1/1	0.325	0.62	0.4

Table 5

Combination of plates	h/h	h/1	1/1
F	0.5	0.1	0.1

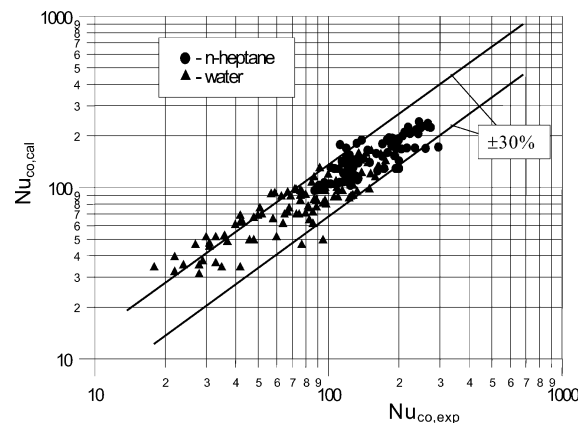


Fig. 11. Comparison of measured and according to Eq. (9) calculated dimensionless heat transfer coefficient Nu_{co} of the condensation process in corrugated plate channel.

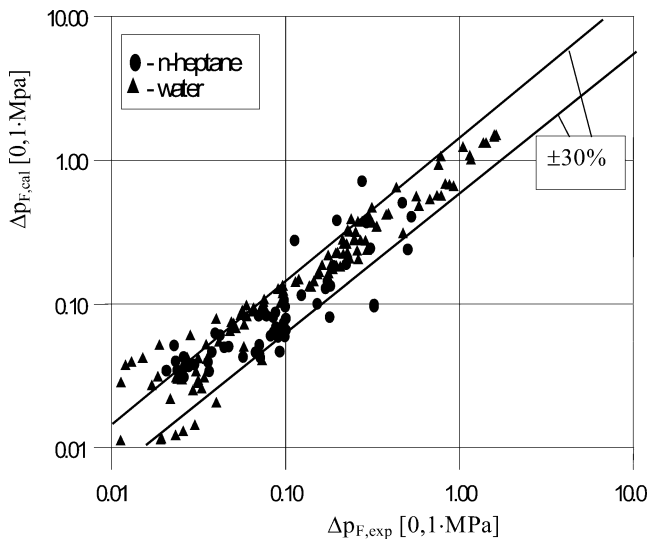


Fig. 12. Comparison of measured and according to Eq. (11) calculated friction pressure drop $\Delta p_{F,co}$ of the condensation process in corrugated plate channel.

In all, the use of experimental data with aqueous and organic condensing phases as well as various geometric conditions is a step to improved general validity.

But, additional experimental data for different systems and various geometric conditions of the corrugated plates and local investigations of the condensing system are necessary for improving the correlations in Eqs. (9) and (11).

5. Conclusion

Experimental investigations in the field of heat transfer and pressure drop were carried out in a vertical 3-channel system with corrugated plates for the conditions of a complete condensation. During the use of the working systems of water and *n*-heptane as well as industrial plate dimensions, the phase loadings and the geometry of the plate corrugation could be determined as essential influence parameters. A plate combination with plates of different corrugation inclination angles (h/l) proves to be an optimal variant in thermic-hydraulic visibility. The model correlations discussed in current literature are of a specific validity. Therefore, they are of limited utility for describing the presented experimental data. The existence of a shear controlled flow regime can be assumed in case of turbulent conditions of the non-adiabatic two-phase system in the narrow corrugated plate channel. Further proposals how to describe the heat transfer and pressure drop of the condensation process in PHE are presented.

References

- [1] B. Thonon, F. Chopard, Condensation in plate heat exchangers: assessment of a general design method, in: Proceedings Eurotherm. Sem. 47th Meeting, Elsevier, Paris, 1996, pp. 10–18.
- [2] K. Stephan, Wärmeübergang beim Kondensieren und beim Sieden, Springer, Berlin, 1988.
- [3] H. Kumar, The design of plate heat exchangers for refrigerants, in: Proc. Inst. of Refrigeration at the Institut of Marine Engineers, London, 6 February, 1992, pp. 50–55.
- [4] Z. Wang, Z. Zhao, Analysis of performance of steam condensation heat transfer and pressure drop in plate condensers, Heat Transfer Engrg. 14 (4) (1993) 32–41.
- [5] C. Panchal, Condensation heat transfer in plate heat exchangers, in: Two-Phase Heat Exchanger Symposium: Present at the 23, National Heat Transfer Conference (ASME), Heat Transfer Division, Heat Transfer Equipment (K-10), New York, 1985, pp. 45–52.
- [6] T. Nakaoka, H. Uehara, Performance test of a shell-and-plate-type condenser for OTEC, Exp. Thermal Fluid Sci. 1 (1988) 275–281.
- [7] L. Di-an, L. Yongren, Steam condensation in a vertical corrugated duct, in: Proceedings of the 1988 National Heat Transfer Conference, vol. 2, in: HTD, vol. 96, ASME, 1988, pp. 389–393.
- [8] C. Tribbe, H. Müller-Steinhagen, The hydrodynamics of gas–liquid two-phase flow in a plate heat exchanger, in: Jubilee Res. Event, Two-Day-Symp. vol. 1, Institution of Chemical Engineers, Rugby, UK, 1997, pp. 357–360.
- [9] G. Kreissig, H. Müller-Steinhagen, Frictional pressure drop for gas–liquid two-phase flow in plate heat exchanger, Heat Transfer Engrg. 13 (4) (1992) 42–52.
- [10] Y. Yan, H. Lio, T. Lin, Condensation heat transfer and pressure drop of refrigerant R-134a in a plate heat exchanger, Internat. J. Heat Mass Transfer 42 (1999) 993–1006.
- [11] L. Tovazhnyanski, P. Kapustenko, Intensification of heat and mass transfer in channels of plate condensers, Chem. Engrg. Commun. 31 (1984) 351–366.
- [12] F. Chopard, C. Marvillet, J. Pantaloni, Assessment of heat transfer performance of rectangular channel geometries: Implications on refrigerant evaporator and condenser, in: Design. Institution of Chemical Engineers Symposium Series 2, Nr. 129 Davis Building, Rugby, UK, Inst. of Chem. Engineering, 1992, pp. 725–733.
- [13] L. Wang, B. Sunden, Pressure drop analysis of steam condensation in a plate heat exchanger, Heat Transfer Engrg. 20 (1) (1999) 71–77.
- [14] L. Wang, R. Christensen, B. Sunden, An experimental investigation of steam condensation in plate heat exchangers, Internat. J. Heat Exchangers 1 (2000) 125–150.
- [15] L. Cheng, T. Chen, Heat transfer and flow friction characteristics of a compact plate-type condenser, in: Proceedings of the ASME, Heat Transfer Division, vol. 3, in: HTD, vol. 361-3; PID, vol. 3, ASME, 1998.
- [16] B. Thonon, A. Bontemps, Condensation of pure and mixtures of hydrocarbons in a compact heat exchanger: experiments and modeling, Heat Transfer Engrg. 23 (6) (2002) 3–17.
- [17] L. Tovazhnyanski, P. Kapustenko, O. Nagoma, The simulation of multicomponent mixtures condensation in plate condensers, in: Proceedings of the International Conference on Compact Heat Exchangers and Enhancement Technology for the Process Industry, third ed., Begell House, New York, 2001, pp. 495–499.
- [18] VDI-Wärmeatlas, 8. Auflage, Mm 1-6, VDI-Verlag, Düsseldorf, 1997.
- [19] B. Thonon, R. Vidil, C. Marvillet, Recent research and developments in plate heat exchangers, J. Enhanced Heat Transfer 2 (1–2) (1995) 149–155.